Dynamics of particle deposition on a disordered substrate. I. Near-equilibrium behavior

Yan-Chr Tsai* and Yonathan Shapir
Department of Physics and Astronomy, University of Rochester, Rochester, New York 14627
(Received 27 April 1994; revised manuscript received 29 July 1994)

A growth model that describes the deposition of particles (or the growth of a rigid crystal) on a disordered substrate is investigated. The dynamic renormalization group is applied to the stochastic growth equation using the Martin, Siggia, and Rose formalism [Phys. Rev. A **8**, 423 (1973)]. The periodic potential and the quenched disorder, upon averaging, are combined into a single term in the generating functional. Changing the temperature (or the inherent noise of the deposition process) two different regimes with a transition between them at T_{sr} are found: for $T > T_{sr}$ this term is irrelevant and the surface has the scaling properties of a surface growing on a flat substrate in the rough phase. The height-height correlations behave as $C(L,\tau) \sim \ln[Lf(\tau/L^2)]$. While the linear response mobility is finite in this phase it does vanish as $(T - T_{sr})^{1.78}$ when $T \to T_{sr}^+$. For $T < T_{sr}$ there is a line of fixed points for the coupling constant. The surface is super-rough: the equilibrium correlation functions behave as $(\ln L)^2$ while their short time dependence is $(\ln \tau)^2$ with a temperature-dependent dynamic exponent $z = 2[1 + 1.78(1 - T/T_{sr})]$. While the linear response mobility vanishes on large length scales, its scale dependence leads to a nonlinear response. For a small applied force F the average velocity of the surface v behaves as $v \sim F^{1+\zeta}$. To first order $\zeta = 1.78(1 - T/T_{sr})$. At the transition, $v \sim F/(1 + C|\ln(F)|)^{1.78}$ and the crossover to the behavior to $T < T_{sr}$ is analyzed. These results also apply to two-dimensional vortex glasses with a parallel magnetic field.

PACS number(s): 05.70.Ln

I. INTRODUCTION

Much progress has been achieved recently in the understanding of surface growth in processes of deposition, sedimentation, epitaxial growth, solidification, etc. [1–3]. A few years earlier the static and the dynamic properties of roughening of crystalline surfaces were elucidated [4,5]. Recent investigations have concentrated on the connections between surface roughening due to thermal fluctuations on one hand and that due to the kinetic growth itself, on the other hand. The underlying discrete structure of the particles (or the lattice) may lead to a kinetic phase transition between smooth and rough phases or between two rough phases with distinct scaling properties [1]. Since the underlying discrete structure is relevant at low temperature (or a low noise regime in the deposition) one cannot escape the question of how disorder in the substrate might modify the surface properties.

The effect of the substrate disorder on the dynamics of the growing surface is the subject of our analysis [6]. We address this issue using the dynamic renormalization group (RG) applied to the stochastic growth equations using the Martin, Siggia, and Rose (MSR) formalism [7].

In the present paper we address the dynamics near equilibrium. This regime is characterized by a very slow rate of deposition such that the system is very close to thermodynamic equilibrium. In this regime only slight modifications from equilibrium are considered. In particular, the fluctuation-dissipation theorem (FDT) [8,9] and the Einstein relation (between the mobility, the diffusion constant, and the temperature) both hold.

Far from equilibrium, the growth equation does not obey the FDT. The symmetry under $h \to -h$ (h is the height of the surface) and time reversal $t \to -t$ are broken. The most relevant additional term, as shown by Kardar, Parisi, and Zhang (KPZ) [10], is due to the lateral growth of the oblique surface. The behavior far from equilibrium will be the subject of a following paper.

In general, the scaling properties of the growing surface are manifested in the height-height correlation function:

$$C(L,\tau) = \langle [h(\vec{x} + \vec{L}, t + \tau) - h(\vec{x}, t)]^2 \rangle \tag{1}$$

or the corresponding surface width:

$$W(L,\tau) = [C(L,\tau)]^{1/2}, \tag{2}$$

which obeys an asymptotic behavior of the form

$$W(L,\tau) = L^{\alpha} f(\tau/L^z). \tag{3}$$

In this expression α is the roughness exponent which characterizes the extent of the roughness of the surface and z is the dynamic exponent. $f(x)$ is a scaling function which approaches a constant for large x. For small x ($\tau \ll L^z$): $f(x) \sim x^{\beta}$ where $\beta = \alpha/z$. At an early stage of the growth the surface roughness increases as

*Present address: Department of Physics and Astronomy, University of Pennsylvania, Philadephia, PA 19104-6396.

$W(\tau) \sim \tau^{\beta}$ while for $\tau \gg L^z$, W depends only on L and behaves as L^{α}.

In the absence of any disorder in the substrate the near-equilibrium behavior was analyzed extensively in the context of surface roughening. The original work was due to Chui and Weeks (CW) [4] and this system was further analyzed by Nozieres and Gallet (NG) [5]. Their most important findings were as follows.

In the high-temperature rough phase

$$C(L,\tau) \sim \ln[Lf(\tau/L^z)] \ , \tag{4}$$

which corresponds to $\alpha = 0$, $\beta = 0$, and $z = 2$. The scaling form of the correlation function in Eq. (3) cannot apply to that of Eq. (4), since both α and β vanish (but with a finite ratio).

In this phase the effect of the discreteness (or the lattice) is not relevant. This behavior is equivalent to that of a free surface in which the surface tension is the only interaction determining its properties.

In this regime the macroscopic mobility defined as the ratio between the average velocity $v = \langle \frac{dh}{dt} \rangle$ and the "force" F driving the surface, is finite.

In the smooth phase $C(L)$ is independent of L, and the mobility vanishes. The mobility has a finite jump from a finite value to zero at the roughening temperature. The growth process at low temperatures is by nucleation of higher "islands" on top of the smooth surface. This "activated" growth has drastically different dynamic properties which are determined by the diffusion of the deposited particles on the surface and their attachment to the "islands."

While we study here the surface properties in deposition of cubic (or tetragonal) rigid particles, our study applies as well to the growth of crystalline surfaces if the rigidity of the solid is large enough. Our theory will apply if the surface height is smaller than the scale on which the random deviations in the substrate cease to affect the positions, along the growth direction, of the lattice ions. This scale will be larger the stronger is the Young's modulus which measures the longitudinal rigidity.

It turns out that the same stochastic equation of motion also describes the behavior of other random two-dimensional (2D) systems. The most important case is a system of vortex lines in a superconducting film with the applied magnetic field parallel to the film. (Charge density waves at finite temperature is another such system.) Therefore the conclusions of our investigations also apply to 2D vortex glasses [11–14]. We shall come back to these implications in the last section.

The outline of this paper is as follows. In Sec. II we present the stochastic equation of growth and the related MSR generating functional. In Sec. III the RG scheme is outlined and the recursion relations are derived. Section IV is devoted to the discussion of the results and their physical implications. The final section, V, is dedicated to a summary of the important conclusions. In the Appendixes we provide more details of the RG calculations. A short Letter announcing the most important results was published elsewhere [6].

II. THE EQUATION OF MOTION AND THE ASSOCIATED GENERATING FUNCTIONAL

The prototypical paradigm for the simplest deposition process is the Edwards and Wilkinson (EW) model [15] for the sedimentation of granular particles. The continuum limit form of their equation of motion for the height $h(\vec{x},t)$ is

$$\tilde{\mu}^{-1}\frac{\partial}{\partial t}h(\vec{x},t) = \nu\nabla^2 h(\vec{x},t) + \tilde{\zeta}(\vec{x},t) + \tilde{F}. \tag{5}$$

$\tilde{\mu}$ is the microscopic "mobility" of the upper surface, ν is the "diffusion constant" for the particles on the surface, $\tilde{F}$ is proportional to the averaged deposition rate which is very small (large deposition rate will be discussed in a second paper), and $\tilde{\zeta}(\vec{x},t)$ is the local fluctuation from the averaged deposition rate, which obeys

$$\langle \tilde{\zeta}(\vec{x},t)\tilde{\zeta}(\vec{x}',t')\rangle = 2\tilde{D}\delta^2(\vec{x}-\vec{x}')\delta(t'-t). \tag{6}$$

We can define the effective "temperature" of this system by the Einstein relation: $T = \tilde{D}\tilde{\mu}$.

If the discrete nature of the particles is taken into account the height h of every column of particles must be an integer multiple of the vertical size of the particle b. This discrete constraint leads to a periodic δ-function potential on h. This periodic potential may be expanded in Fourier series of which only the basic harmonic is relevant. On a flat substrate there will be an additional term of the form $\gamma\frac{\tilde{y}}{a^2}\sin[\gamma h(\vec{x},t)]$ on the right hand side of Eq. (5) ($\gamma = \frac{2\pi}{b}$ and $\frac{\tilde{y}}{a^2}$ is the amplitude of the periodic potential).

In the presence of a random substrate the minima of the potential will be randomly, and independently, shifted for each column. Hence the equation of motion becomes

$$\tilde{\mu}^{-1}\frac{\partial}{\partial t}h(\vec{x},t) = \nu\nabla^2 h(\vec{x},t) + \gamma\frac{\tilde{y}}{a^2}\sin\{\gamma[h(\vec{x},t)+d(\vec{x})]\} + \tilde{\zeta}(\vec{x},t) + \tilde{F} \ . \tag{7}$$

$d(\vec{x})$ is the local deviation of the disordered substrate as depicted in Fig. 1. The associated "phase" $\Theta(\vec{x}) = \frac{2\pi d(\vec{x})}{b}$ is uniformly distributed between 0 and 2π, and is uncorrelated for different locations $\vec{x}$ on the substrate.

Then the equation of the growth process becomes

$$\tilde{\mu}^{-1}\frac{\partial h(\vec{x},t)}{\partial t} = \tilde{F} + \nu[\nabla^2 h(\vec{x},t)] + \frac{\gamma\tilde{y}}{a^2}\sin[\gamma h(\vec{x},t) + \Theta(\vec{x})] + \tilde{\zeta}(\vec{x},t), \tag{8}$$

where a is the lattice constant in the horizontal plane.

To investigate this stochastic equation systemically, one can utilize the Martin, Siggia, and Rose formalism [7] by introducing an auxiliary field $\tilde{h}$ to force Eq. (8) through a functional integral representation of a δ function. The generating functional for Eq. (8) takes the form as [after averaging over $\zeta(\vec{x},t)$]

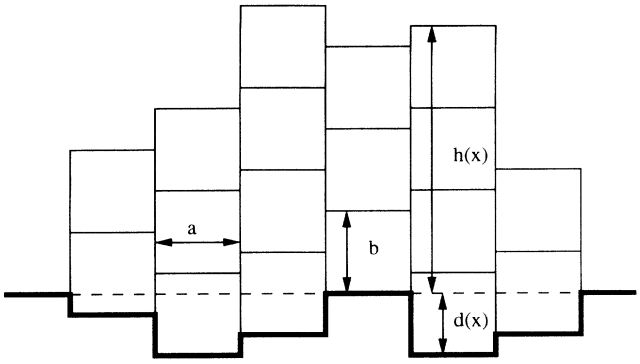

FIG. 1. A two-dimensional cut (along a lattice plane perpendicular to the disordered substrate) of the three-dimensional system.

$$Z_\Theta[\tilde{J},J]=\int \mathcal{D}\tilde{h}\mathcal{D}h\exp\Bigg(S_0[\tilde{h},h] +S_I[\tilde{h},h]+\int d^2xdt(\tilde{J}\tilde{h}+Jh)\Bigg), \tag{9}$$

where

$$S_0[\tilde{h},h]=\int d^2xdt\left[\tilde{D}\tilde{\mu}^2\tilde{h}^2-\tilde{h}\left(\frac{\partial}{\partial t}h-\tilde{\mu}\nu\nabla^2h\right)\right], \tag{10}$$

$$S_I=\int d^2xdt\left(\frac{\tilde{\mu}\gamma\tilde{y}}{a^2}\tilde{h}\sin[\gamma h(\vec{x},t)+\Theta(\vec{x})]\right). \tag{11}$$

The generating functional $Z[J,\tilde{J}]$ can be directly averaged over the quenched disordered $d(\vec{x})$ because $Z[J=\tilde{J}=0]=1$ [20]. One may calculate any averaged correlation and response function by differentiating the generating functional with respect to the current J or auxiliary current $\tilde{J}$ and setting $J=\tilde{J}=0$.

After averaging over the disorder the effective generating functional reads

$$\langle Z_\Theta[\tilde{J},J]\rangle_{disorder}=\int \mathcal{D}\tilde{h}\mathcal{D}h\exp\Bigg\{\int d^2xdt\left[\tilde{D}\tilde{\mu}^2\tilde{h}^2-\tilde{h}\left(\frac{\partial}{\partial t}h-\tilde{\mu}\nu\nabla^2h\right)\right] +\frac{\tilde{\mu}^2\gamma^2\tilde{g}}{2a^2}\int\int d^2xdtdt'\tilde{h}(\vec{x},t)\tilde{h}(\vec{x},t')\cos\{\gamma[h(\vec{x},t)-h(\vec{x},t')]\}\Bigg\}, \tag{12}$$

where $\tilde{g}=\tilde{y}^2$. If we choose $\tilde{D}=T\tilde{\mu}^{-1}$, the system will evolve into the configurations weighted by a Boltzmann factor $e^{-H/T}$, which obeys the fluctuation-dissipation theorem [8]. To simplify the calculation, we redefine those physical parameters as $\tilde{\mu}\nu=\mu,\tilde{D}\nu^{-2}=D,\tilde{g}=g\nu^2,\tilde{\nu}=\bar{\nu}\nu^2$, $F=\frac{\bar{F}}{\nu}$. Then the equation of motion becomes

$$\mu^{-1}\frac{\partial h(\vec{x},t)}{\partial t}=F+[\nabla^2h(\vec{x},t)]+\frac{\gamma y}{a^2}\sin[\gamma h(\vec{x},t)+\Theta(\vec{x})]+\zeta(\vec{x},t). \tag{13}$$

Here $\langle\zeta(\vec{x_1},t_1)\zeta(\vec{x_2},t_2)\rangle=2D\delta^{(2)}(\vec{x_1}-\vec{x_2})\delta(t_1-t_2)$. The resulting generating functional for the present case reads

$$Z_\Theta[\tilde{J},J]=\int \mathcal{D}\tilde{\phi}\mathcal{D}\phi\exp\left(S_0[\tilde{\phi},\phi]+S_I[\tilde{\phi},\phi]+\int d^2xdt(\tilde{J}\tilde{\phi}+J\phi)\right), \tag{14}$$

where

$$S_0[\tilde{\phi},\phi]=\int d^2xdt\left[D\mu^2\tilde{\phi}^2-\tilde{\phi}\left(\frac{\partial}{\partial t}\phi-\mu\nabla^2\phi\right)\right], \tag{15}$$

$$S_I=\int d^2xdt\left(\frac{\mu\gamma y}{a^2}\tilde{\phi}\sin[\gamma\phi(\vec{x},t)+\Theta(\vec{x})]\right), \tag{16}$$

where $h(\vec{x},t)=\phi(\vec{x},t)$ and $\tilde{h}(\vec{x},t)\sim\tilde{\phi}(\vec{x},t)$. In the same way, we arrive at the averaged effective generating functional:

$$\langle Z_\Theta[\tilde{J},J]\rangle_{disorder}=\int \mathcal{D}\tilde{\phi}\mathcal{D}\phi\exp\Bigg\{\int d^2xdt\left[D\mu^2\tilde{\phi}^2-\tilde{\phi}\left(\frac{\partial}{\partial t}\phi-\mu\nabla^2\phi\right)\right] +\frac{\mu^2\gamma^2g}{2a^2}\int\int d^2xdtdt'\tilde{\phi}(\vec{x},t)\tilde{\phi}(\vec{x},t')\cos\{\gamma[\phi(\vec{x},t)-\phi(\vec{x},t')]\}\Bigg\}. \tag{17}$$

In the generating functional in Eq. (17), the term which contains the $\cos[\gamma(\phi(\vec{x},t)-\phi(\vec{x},t')]$ is nonlocal in time and will be responsible for the creation of nontrivial Edwards-Anderson correlations.

In the renormalization process it turns out that this term generates a new "quadratic" term, also nonlocal in time, of the form

$$\frac{1}{2}\mu^2\bar{\nu}\int dxdtdt'\nabla\tilde{\phi}(x,t)\nabla\tilde{\phi}(x,t') \ . \tag{18}$$

We therefore add this term to the generating functional and will follow the flow of $\bar{\nu}$ as well (as shown below it will play a crucial role in altering the long-range height-height correlations).

Here we treat the last term in Eq. (17) as a perturbation to the free action, and expand the theory in orders of g and $\delta(=\frac{\gamma^2 D\mu}{4\pi}-1)$. The RG scheme will be discussed in the next section and details are given in the Appendixes.

III. THE RENORMALIZATION SCHEME AND THE RECURSION RELATIONS

The renormalization group scheme we follow is based on the sine-Gordon field theory developed by Amit *et al.* [16]. The extension to the dynamics was performed by Goldschmidt and Schaub (GS) [17]. Since they presented many details of their calculations, we shall not repeat them here. Rather we only outline the approach and provide Appendixes with detailed explanations which complement these given by GS.

The following renormalization constants are defined through the relations between the bare and the renormalized couplings:

$$D_0 = Z_D D, \quad g_0 = Z_g g, \tag{19}$$

$$m_0^2\phi^2 = m^2\phi_R^2, \quad \gamma_0^2\phi^2 = \gamma^2\phi_R^2,$$
$$\phi^2 = Z_\phi\phi_R^2, \quad \tilde{\phi}^2 = (\tilde{Z}_{\tilde{\phi}})\tilde{\phi}_R^2, \tag{20}$$

$$\mu_0 = (Z_{\tilde{\phi}}Z_\phi^{-1})^{-\frac{1}{2}}\mu. \tag{21}$$

The subscript R labels the renormalized field variable, and 0 the bare variable or the coupling constant.

For convenience, we define $\tilde{Z}_{\tilde{\phi}} = [Z_{\tilde{\phi}}]^2$.

The renormalization of μ depends on Z_ϕ and $Z_{\tilde{\phi}}$, and no additional Z factor for renormalization is required. This is due to the FDT, which implies

$$-\theta(t)\frac{d}{dt}\langle\phi(x,t)\phi(0,0)\rangle = \mu\langle\phi(x,t)\tilde{\phi}(0,0)\rangle. \tag{22}$$

Here $\theta(t)$ equals 1 for $t > 0$, and 0 for $t < 0$. Equation (21) is obtained by substituting Eq. (20) into Eq. (22). As we will show later, $D\mu$ will not suffer any renormalization. Therefore it is not necessary to calculate Z_D in the harmonic model, which obeys the FDT.

As outlined by GS, the model has a very important symmetry, $\phi(\vec{x},t) \to \phi(\vec{x},t) + f(x)$, where $f(x)$ is an arbitrary spatial function constant in time. As a result $\phi(\vec{x},t)$ cannot be renormalized and $Z_\phi = 1$ [17] to all orders in g.

We also mention that the lattice effects and the quenched disorder in the substrate violate the Galilean symmetry, which provides another Ward identity $z+\alpha = 2$ [10] for the system without these effects.

The calculations of the Z factors are exemplified in the Appendixes, in which the explicit calculations of some of them are given.

A. Recursion relations

Once the Z factors are known to the leading order in g, the recursion relations are obtained via the so-called β functions [18–20]:

$$\beta_\mu = \kappa\left(\frac{\partial\mu}{\partial\kappa}\right)_b = \mu\kappa\left(\frac{\partial\ln Z_{\tilde{\phi}}}{\partial\kappa}\right)_b = \left(\frac{g\gamma^2\sqrt{c}}{D\mu}\right)\mu, \tag{23}$$

$$\beta_D = \kappa\left(\frac{\partial D}{\partial\kappa}\right)_b = -D\kappa\left(\frac{\partial\ln Z_D}{\partial\kappa}\right)_b = \left(-\frac{\gamma^2 g\sqrt{c}}{D\mu}\right)D, \tag{24}$$

$$\beta_g = \kappa\left(\frac{\partial g}{\partial\kappa}\right)_b = -g\kappa\left(\frac{\partial\ln Z_g}{\partial\kappa}\right)_b = 2\delta g + \frac{2\pi g^2}{(D\mu)^2}, \tag{25}$$

$$\beta_{\bar{\nu}} = \kappa\left(\frac{\partial\bar{\nu}}{\partial\kappa}\right)_b = -\frac{\pi\gamma^2}{4(D\mu)^2}g^2, \tag{26}$$

where subscript b means that all bare parameters are fixed when one performs the differentiations [18–20] and κ is a mass scale. The renormalization of the couplings may also be related to the same β functions. Their flow under a scale change by a factor $b = \exp(l)$ is given by minus the related β function, in addition to the naive dependence which originates in the rescaling of $x \to bx$ $k \to b^{-1}k$, and $t \to b^z t$. The recursion relations so obtained are as follows:

$$\frac{d\nu}{dl} = 0, \tag{27}$$

$$\frac{d\tilde{\nu}}{dl} = \frac{\pi\gamma^2}{4\nu(\tilde{D}\tilde{\mu})}\tilde{g}^2, \tag{28}$$

$$\frac{d\tilde{D}}{dl} = \left(2-z+\frac{\tilde{g}\gamma^2\sqrt{c}}{\tilde{D}\tilde{\mu}\nu}\right)\tilde{D}, \tag{29}$$

$$\frac{d\tilde{\mu}}{dl} = -\left(2-z+\frac{\tilde{g}\gamma^2\sqrt{c}}{\tilde{D}\tilde{\mu}\nu}\right)\tilde{\mu}, \tag{30}$$

$$\frac{d\tilde{g}}{dl} = \left(2-\frac{\gamma^2\tilde{D}\tilde{\mu}}{2\pi\nu}\right)\tilde{g} - \frac{2\pi}{(\tilde{D}\tilde{\mu})^2}\tilde{g}^2. \tag{31}$$

In the next section we discuss the asymptotic scaling behaviors implied by these flow equations.

IV. DISCUSSION

Recalling that the temperature of the system is $T = \tilde{D}\tilde{\mu}$, we find that $\frac{\partial T}{\partial l} = 0$. Hence the temperature is not renormalized. The behavior of the system is governed by the renormalization of the coupling g. The flow of $\tilde{g}$ depends crucially on the temperature. Let us define $T_{sr} = \frac{\nu b^2}{\pi}$. The recursion relation for $\tilde{g}$ takes the form

$$\frac{\partial \tilde{g}}{\partial l} = 2\left(1 - \frac{T}{T_{sr}}\right)\tilde{g} - \frac{2\pi}{T^2}\tilde{g}^2. \tag{32}$$

Therefore for $T > T_{sr}$ $\tilde{g}$ flows to zero, while for $T < T_{sr}$ $\tilde{g}$ flows to a fixed point of order $-\delta = 1 - \frac{T}{T_{sr}}$ with a continuous line of fixed points (see Fig. 2).

We now analyze the dynamics in each phase separately.

A. The high-temperature phases: $T > T_{sr}$

Since $\tilde{g} \to 0$ in this phase the equilibrium properties are the same as in the high-temperature rough phase if a surface on a smooth substrate $C(L) \sim \frac{T}{\nu}\ln(L)$.

Way above T_{sr} the mobility of the surface is finite. However, as T_{sr} is approached the mobility becomes smaller and eventually vanishes at $T = T_{sr}$.

Integrating the recursion relation we find that

$$\tilde{\mu} \sim \tilde{\mu}_0 \left(\frac{T}{T_{sr}} - 1\right)^{2\sqrt{c}}, \tag{33}$$

with $2\sqrt{c} = 1.78$.

The dynamic exponent remains $z = 2$ throughout this phase, although the asymptotic scaling behavior is reached only on scales $L > L_g$ where $L_g \sim g_0^{\frac{-1}{2\delta}}$ is the scale on which $\tilde{g}$ decays to zero. The scale L_g diverges as $T \to T_{sr}$ since $\ln(L_g) \sim (\frac{T}{T_{sr}} - 1)^{-1}$.

As long as one sits at a temperature $T > T_{sr}$, the decay of $\tilde{g}$ under the flow will not alter the asymptotic scaling behavior for $L > L_g$, except that the amplitude in the correlation function depends on the bare value of $\tilde{g}$.

In the high-temperature phase, the flow of $\tilde{\mu}(l)$ can be calculated in terms of $\tilde{g}(l)$:

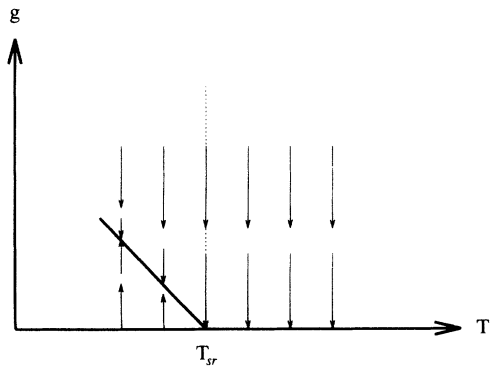

FIG. 2. The flow diagram for $g(l)$ with two different fixed lines for T larger and smaller than T_{sr}.

$$\tilde{\mu}(l) = \tilde{\mu(0)}e^{-\beta\int_0^l \tilde{g}(l')dl'}, \tag{34}$$

where $\beta = \frac{\gamma^2\sqrt{c}}{\tilde{D}\tilde{\mu}\nu}$, and

$$\tilde{g}(l) = \frac{-\delta\tilde{g}(0)e^{-\delta l}}{-\delta - \alpha\tilde{g}(0) + \alpha\tilde{g}(0)e^{-\delta l}}, \tag{35}$$

with $\alpha = \frac{2\pi}{(\tilde{D}\tilde{\mu})^2}$.

Now we can obtain the macroscopic mobility, $\tilde{\mu} \sim \tilde{\mu}(l \to \infty)$, in the linear response regime ($F \to 0$) for the high-temperature phase.

$$\tilde{\mu}(l = \infty) = \tilde{\mu}(l = 0)\left(\frac{|\delta|}{\alpha\tilde{g}(0) + |\delta|}\right)^{\beta/\alpha} \sim |\delta|^{\beta/\alpha}, \tag{36}$$

where $\frac{\beta}{\alpha} = 2\sqrt{c} \sim 1.78$.

As $T \to T_{sr}^+$, μ_M vanishes continuously as demonstrated above. In the low-temperature phase $\tilde{g}(l)$ flows to a finite value. Its fixed-point location changes with the temperature. More explicitly, the set of fixed points of different temperatures forms a fixed line in the plane of $\tilde{g}$ and T, in which $\tilde{g}^*(T) \sim T_{sr} - T$, to first order. In this phase the scaling equilibrium properties and the dynamics, as well as the transport properties, are drastically modified. Most of the forthcoming discussions are devoted to this new, super-rough phase.

B. The low-temperature ($T < T_{sr}$) super-rough phase

The regime of temperatures below the transition provides the most exciting new physics. The theoretical predictions which follow are: (i) The correlations will change from $C(L) \sim \ln L$ to $C(L) \sim (\ln L)^2$. Hence the surface is even rougher than that in the rough phase at $T > T_{sr}$. This behavior was dubbed by Toner and DiVincenzo as super-rough [21]. They found it first in the surface of crystals with bulk disorder. (ii) The dynamic critical exponent z now displays a temperature dependence. It increases continuously from its value above T_{sr}, $z = 2$, and $z - 2$ is to first order linear in $T_{sr} - T$. (iii) The linear response macroscopic mobility vanishes. The response becomes nonlinear [5], at least close to the transition, such that the average velocity v scales with the external force $\tilde{F}$ as $v \sim \tilde{F}^{\eta+1}$, where η is also a temperature-dependent exponent (related by scaling to the dynamic exponent z).

In the following we concentrate on each of these physical manifestations separately.

1. Super-rough equilibrium correlations

For $T_{sr} > T$, g approaches a line of fixed points $\tilde{g}^* = (T_{sr} - T)/\pi$ (see Fig. 2). As was shown by Toner and DiVincenzo [21], the correlation function of the 2D surface acquires a second logarithmic factor. Since they used the static replica formalism for a model with bulk disorder, we explain here how this behavior is obtained within the dynamics formulation, for the case of disorder

in the substrate.

The Fourier transformation of $C(L,0)$ two-point vertex function $\Gamma_{0,2}(q,t=0)$ is defined as before:

$$\Gamma_{0,2}(q,t=0) = \langle\langle h(q)h(-q)\rangle\rangle_{disorder}. \tag{37}$$

For systems with vanishing g, $\Gamma_{0,2}(q) = \frac{1}{\nu q^2}$. Once the term $\bar{\nu}\int\int\int dxdtdt' \nabla\tilde{h}(\vec{x},t)\ \nabla\tilde{h}(\vec{x},t')$ has to be accounted for, the height-height correlation functions are obtained from the quadratic part of the Hamiltonian which contains this term. One obtains the equal-time dynamic correlation (namely, the static correlation function),

$$\Gamma_{0,2}(q,t=0) = \frac{1}{\nu q^2} + \frac{\bar{\nu}q^2}{(\nu q^2)^2}. \tag{38}$$

The first term is the equal-time correlation originating from the time-dependent part of the correlation. The second term arises from the so-called time-persistent part, which will be explained in Appendix A.

The second term is proportional to $\frac{1}{q^2}$ as the first. However, because $\bar{\nu}(l)$ increases with l (while ν remains unchanged with l), it carries another scale dependence. The height-height correlation function, under a scale transformation by the factor $b = e^l$ changes as

$$\begin{aligned}\langle h(\vec{q})h(-\vec{q})\rangle &= \Gamma_{0,2}(\vec{q};\nu,\bar{\nu}(0),g(0)) \\ &= e^{2l}\Gamma_{0,2}[e^l\vec{q};\nu,\bar{\nu},g(l)].\end{aligned} \tag{39}$$

The first term in Eq. (39) comes from the naive dimension of $\langle h(\vec{q})(-\vec{q})\rangle$. Using Eq. (38) with the renormalized values one obtains

$$\langle h(\vec{q})(-\vec{q})\rangle = e^{2l}\frac{1}{\nu e^{2l}q^2}\left(1+\frac{\bar{\nu}(l)}{\nu}\right) = \frac{1}{\nu q^2}\left(1+\frac{\bar{\nu}(l)}{\nu}\right). \tag{40}$$

Apart from a finite part, $\bar{\nu}(l)$ increases as $\sim (g^*)^2 l$. By choosing l such that $e^l q = \Omega = a^{-1}$ (where Ω, the momentum cutoff, can be chosen as the inverse lattice spacing), the vertex function, $\Gamma_{0,2}(q,t=0)$, is found as

$$\Gamma_{0,2}(q,t=0) = \frac{1}{\nu q^2}\left(A - B\frac{(g^*)^2}{\nu}\ln(qa)\right), \tag{41}$$

where $A=1, B=\frac{\pi\gamma^2}{4\nu^2}$. Consequently the static correlation function is

$$C(L) = A'\ln\left(\frac{L}{a}\right) + B'\ln^2\left(\frac{L}{a}\right). \tag{42}$$

Hence the behavior found by Toner and DiVincenzo [21] for the bulk disorder is also reproduced in the system under consideration, where only the substrate is disordered. Experimentally, it might be difficult to distinguish $\ln(\frac{L}{a})$ from $\ln^2(\frac{L}{a})$. However, the dynamical behavior in both phases is apparently different and their difference may be detected by the experimental observations.

The behavior found above persists in the regime $L \ll \tau^{1/z}$.

For $L \gg \tau^{1/z}$ simple scaling implies a dependence of $(\ln\tau)^2$ on τ. The derivation of the intermediate behavior of $C(L,\tau)$ is beyond the scope of this paper [it requires the knowledge of $\Gamma_{0,2}(\vec{q},\omega)$]. However, simple physical considerations hint very strongly that its behavior is of the form $C(L,\tau) \sim \{\ln L f[\tau/L^z]\}^2$.

2. The dynamic exponent

To calculate the value of the dynamic exponent z in the low-temperature phase one should look at the recursion relations of $\tilde{D}$ and $\tilde{\mu}$. To locate the fixed point one can require that both of $\frac{d\tilde{D}}{dl}$ and $\frac{d\tilde{\mu}}{dl}$ be equal to zero. Then z is obtained as $z = 2 + 4\sqrt{c}|\delta|$, where the fixed-point value of g, $g^* = \frac{-\delta}{\pi}$, was inserted. As far as we know, this is the first example in which the dynamic exponent z varies with temperature continuously (besides the random anisotropy XY model which is described by a similar field theory [17]). The physical implications of the increasing z can be understood from the fact that the relaxation time to reach the equilibrium state is longer as the temperature is lowered below T_{sr}. This is to be expected in the phase where the disorder is relevant, and the surface turns super-rough as explained in the preceding section. Since the surface stretches itself to find the configurations with the lower free energy, it will leave these locations slowly. The slower dynamics implies also a graduated increase in the averaged free energy $F(L)$ barriers, associated with a scale L, due to the disorder.

3. The nonlinear response

In the last section, addressing the high-temperature rough phase, we have found that the linear response mobility vanishes as $(T-T_{sr})^{1.78}$, when T is reduced to T_{sr}. Below T_{sr} the linear response mobility $\tilde{\mu}_M$ vanishes.

As we show in the following the response becomes nonlinear. Again the physical origin of this behavior takes roots in the preferred configurations of the surface which are local minima of its free energy. Applying a small force F will not move the surface in a uniform velocity. Actually a somewhat similar situation occurs in the smooth phase of a surface growing upon a flat substrate, where the mobility jumps from a finite value to zero at the roughening temperature.

If the pinning is even stronger the surface grows by activation of higher islands. If the substrate is disordered, the preferred and inhomogeneous locations of the surface are enough to slow the motion and then to cause the linear response mobility to vanish. However, it still allows for a uniform motion with average velocity which vanishes as $\tilde{F}^{1+\eta}$ ($\eta > 0$) when $\tilde{F} \to 0$. Hence the velocity vanishes faster than $\tilde{F}$. The force $\tilde{F}$ is a relevant field which increases as $\tilde{F}(L) \sim \tilde{F}_0 L^2$ with the length scale. Even for small $\tilde{F}_0$ there is a scale $L^* \sim aF_0^{-1/2}$ for which the scaled force is of order 1, namely, it is not a neg-

ligible quantity. On the scale, $L > L^*$ the behavior is not "critical." The large force moves the surface with a uniform velocity. The ratio between the force and the velocity is determined by the mobility μ at the boundary L^* between the "critical" ($L < L^*$) and the "noncritical" ($L > L^*$) regimes. Within the scaling picture L^* can serve as a "cutoff length." Hence it is the mobility $\mu(L^*)$ for a piece of the interface with linear extent L^* that is determining the mobility of the whole surface on scales $L > L^*$. Note that $\tilde{\mu}(L)$ is not exactly $\tilde{\mu}(L^*)$ but the ratio between them is finite since no "critical scaling" holds for $L > L^*$. The scaling of $\tilde{\mu}(L)$ for $L < L^*$ may be derived from its definition as

$$\frac{\partial h}{\partial t} = \mu F. \tag{43}$$

Under rescaling $L \to L/b$ we already know that $t \to t/b^z$ and $F \to Fb^2$ while h does not suffer any renormalization. To make both sides scale similarly we must have $\mu \to \mu b^{2-z}$ and defining $\mu \sim \mu_0 b^{-2\eta}$ we obtain

$$\eta = (z-2)/2 = -2\sqrt{c}\delta = 1.78|\delta| \ . \tag{44}$$

That implies that $\mu(L)$ on a scale $L < L^*$ is made smaller by $(\frac{L}{a})^{-2\eta}$ with respect to its bare value. In particular, we find

$$\mu(L^*) = \mu_0 \left(\frac{L^*}{a}\right)^{-2\eta} = \mu_0 F_0^{\eta} = \mu_0 F_0^{z/2-1}, \tag{45}$$

where we have used the relation between L^* and F_0.

So we have identified the dependence of μ_M on F_0 from which we obtain the averaged velocity:

$$v \sim \mu_0 F_0^{\eta} F_0 = \mu_0 F_0^{1+\eta} = \mu_0 F_0^{z/2}. \tag{46}$$

Thus as temperature is lowered the velocity (for the same tiny force F_0) becomes smaller. How far below T_{sr} do these relations hold? The scaling picture is based on a local equation of motion of h. Therefore it implicitly assumes the existence of a single solution for the equation of motion in the limit of vanishing uniform force. Just below T_{sr} this is a valid assumption since even if more than one minima exists the scale associated with the difference between the minimizing configurations (which diverges as $T \to T_{sr}$) is larger than the scale we discussed here. At lower temperature this may no longer hold. The existence of multiple minima might be felt on the relevant scale (i.e., L^*). In the regime where many minima are relevant the dynamics will be activated. In other words, the slower processes are going to be related to the height of the barriers between these minima. Some works [22,13] have been devoted to estimating these barriers and drawing the conclusions based on "activated dynamics." It is not clear, however, how reliable these heuristic estimates are (e.g., the barriers are identified with the fluctuation in the minima of the free energy). Unbounded barriers between configuration unrelated by symmetry will also lead to broken ergodicity which can be reflected in "replica symmetry breaking." Such a possibility was found recently within a variational approach [23].

C. T at and just below T_{sr}

The discussion we presented so far for $T < T_{sr}$ applies on length scales for which $\tilde{g}$ is already close to its fixed-point value $\tilde{g}^*$. If the temperature is very close to T_{sr} these scales become very large and it will be necessary to account for the crossover regime. The recursion relations can be integrated as before and yield, for the scale-dependent mobility,

$$\tilde{\mu}(l) = \tilde{\mu}(0)\left\{1 + \frac{4\pi}{T^2}\tilde{g}(0)\frac{1}{2|\delta|}\left[\left(\frac{L}{a}\right)^{2|\delta|} - 1\right]\right\}^{-2\sqrt{c}}. \tag{47}$$

From this expression we see that if $(\frac{L}{a})^{2|\delta|} \gg 1$ the results of the preceding section apply. If the force $\tilde{F}$ is not small enough for the associated scale L^* to satisfy this condition the relation between the velocity and the applied force changes to

$$v/F \sim \left(1 + \frac{4\pi\tilde{g}(0)}{T^2}\frac{1}{2\delta}(\tilde{F}^{-|\delta|} - 1)\right)^{-1.78}. \tag{48}$$

At $T = T_{sr}(\delta = 0)$ this expression yields

$$\frac{v}{F} \sim \left(1 + \frac{2\pi g(0)}{T^2}\ln(F)\right)^{-1.78}, \tag{49}$$

namely, v/F vanishes as $F \to 0$ due to logarithmic corrections. They originate from the effect of g which is marginally irrelevant and decays to zero so slowly that it still causes v/F to vanish.

V. SUMMARY

To summarize the main conclusions of our investigation on the effect of disorder in the substrate on the surface dynamics: There exists a phase transition between a high-temperature, rough phase, and a low-temperature, super-rough phase.

In the rough phase correlations and response functions have the same scaling properties as in the pure case. The disorder and the periodic potential are irrelevant in this phase. As the transition temperature T_{sr} is approached from above the macroscopic mobility vanishes continuously as $(T - T_{sr})^{1.78}$ (contrary to the flat substrate in which it has a finite jump).

The properties of the low-temperature phase are unique. The height-height correlations are $C(L,\tau) \sim [\ln L]^2$ as $L \ll \tau^{1/z}$, and $C(L,\tau) \sim [\ln \tau]^2$ as $L \gg \tau^{1/z}$ with $z = 2 + 4\sqrt{c}(1 - \frac{T}{T_{sr}})$ to first order in $(1 - T/T_{sr})$, namely, the dynamic exponent increases continuously from its Gaussian value of 2 as the temperature is lowered below the transition.

The linear mobility has a scale dependence which causes it to vanish on a large scale. We have shown that this scale dependence results in a nonlinear relation between the applied force and the average velocity: $v \sim F^{1+\eta}$, where $\eta = 1.78(1 - \frac{T}{T_{sr}})$ is also a temperature-

dependent exponent.

All these results also apply to the 2D vortex-glass system in a film of type-II superconductors.

We discussed these implications elsewhere [14]. The most important one is the nonlinear relation between the voltage V and the current I: $V \sim I^{1+\eta}$ with η given above.

Our RG calculations give the same static behavior as obtained by the replica approach with unbroken replica symmetry.

Other works have shown the symmetry to be broken within a nonperturbative variational harmonic approximation which is equivalent to the $N \to \infty$ limit. It is still unsettled whether the replica symmetry is indeed broken for $N = 1$.

Preliminary numerical results for a 2D vortex-glass [27] and a random growth model [28] show a transition in the dynamic properties at a temperature within 10% of the analytic RG result. Looking at the static correlations below T_{sr}, however, the possibility of the replica-symmetry breaking may not be excluded. However, it is too early to draw firm conclusions from those preliminary results. It is to be expected, therefore, that more analytical and numerical works would be necessary to reconcile the different results and to reach a complete understanding of this exciting and challenging problem.

ACKNOWLEDGMENTS

We are thankful to M. Kardar, G. Grinstein, B. Schmittmann, T. Giamarchi, and especially to D. Huse for most useful discussions. We are also indebted to Y. Goldschmidt for bringing to our attention Ref. [17]. We are also grateful to D. Cule and T. Hwa for sharing with us their numerical results. Acknowledgment is also made to the donors of The Petroleum Research Fund, administered by the ACS, for support of this research.

APPENDIX A: RESPONSE AND CORRELATION FUNCTIONS

Two kinds of propagators, the response function and the correlation function, arise from the free (Gaussian) portion in the effective action in Eq. (17) (consisting of a quadratic form in the field ϕ and the auxiliary field $\tilde{\phi}$). One can calculate the free response and correlation functions directly from the free part of the action S_0 in Eq. (15). In the momentum and frequency representation, they are

$$\langle \phi(\vec{q},\omega)\tilde{\phi}(-\vec{q},-\omega)\rangle = \frac{1}{\mu(q^2+m^2)+i\omega}, \tag{A1}$$

$$\langle \phi(\vec{q},\omega)\phi(-\vec{q},-\omega)\rangle = \frac{2D\mu^2}{[\mu(q^2+m^2)]^2+\omega^2}, \tag{A2}$$

where m is the mass of the field ϕ. We have introduced the mass m to regularize the infrared divergences which appear in the upcoming loop calculations. In the momentum and time representation, they are given by

$$\langle \phi(\vec{q},t)\tilde{\phi}(-\vec{q},t')\rangle = \theta(t-t')e^{-\mu(q^2+m^2)(t-t')}, \tag{A3}$$

$$\langle \phi(\vec{q},t)\phi(-\vec{q},t')\rangle = \frac{D\mu}{q^2+m^2}e^{-\mu(q^2+m^2)|t-t'|}. \tag{A4}$$

In this manner, both the free response and free correlation functions possess a mass dependence in their denominators as one can see from Eqs. (A1)–(A4).

The short-distance cutoff is introduced for regularizing the ultraviolet divergence in two dimensions. The regularized C_0 and R_0 are

$$C_0(\vec{x},t) = \int \frac{d^2\vec{q}}{(2\pi)^2} e^{i\vec{q}\cdot\vec{y}-\mu(q^2+m^2)} \frac{D\mu}{q^2+m^2}\bigg|_{y^2=x^2+a^2}, \tag{A5}$$

$$R_0(\vec{x},t) = \frac{\theta(t)}{4\pi\mu t} e^{-\frac{x^2+a^2}{4\mu t}-m^2\mu t}. \tag{A6}$$

Furthermore, the following equations are very valuable to extract the asymptotic behavior of free propagators [17]:

$$\bar{C}_0(x,t) \sim -\frac{1}{4\pi}\ln(m_0^2\lambda_0|t|) - \frac{1}{4\pi}C - \frac{1}{4\pi}\frac{x^2+a^2}{4\lambda|t|},$$

$$\text{as } m^2(x^2+a^2) \ll m_0^2\lambda|t| \ll 1, \tag{A7}$$

$$\bar{C}_0(x=0,t) = -\frac{1}{4\pi}\ln(2\sqrt{c}m_0^2\lambda|t|) + O\left(\frac{a^2}{\lambda_0|t|}\right), \tag{A8}$$

where $C_0(\vec{x},t) = D\mu\bar{C}_0(\vec{x},t)$, and C is Euler's constant ≈ 0.5772. In the limit $m_0^2\lambda|t| \ll m^2(x^2+a^2) \ll 1$, the equal-time correlation behaves as

$$\bar{C}_0(x,t=0) = -\frac{1}{4\pi}\ln[cm_0^2(x^2+a^2)] + O(x^2). \tag{A9}$$

The zero-order fluctuation-dissipation theorem relates the response function to the correlation function as follows:

$$-\frac{1}{\mu^2 D}\theta(t)\frac{d}{dt}C_0(\vec{x},t) = R_0(\vec{x},t). \tag{A10}$$

(1) *Basic diagrams.* In Fig. 3 the wavy line represents the auxiliary field $\tilde{\phi}$; the straight line represents the field ϕ. The dashed line is set to separate two different time coordinates. The dot points represent the abbreviation of the other ϕ lines.

(2) *Free propagators.* Correlation function $C_0(\vec{x},t)$ and response function $R_0(\vec{x},t)$ are shown in Fig. 4.

In general, the equal-time correlation function, $C(\vec{x},t=0) = \langle \phi(\vec{x},t)\phi(0,t)\rangle$, is identical to the static correlation function $\langle \phi(x)\phi(0)\rangle$ averaged by the Boltzmann weight. As a special case for the connection, one can refer to Eq. (A4). On the other hand, the response

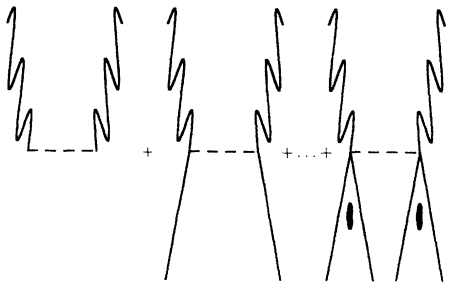

FIG. 3. The Feynman diagram representing $\tilde{\phi}(\vec{x},t)\tilde{\phi}(\vec{x},t')\cos[\phi(\vec{x},t)-\phi(\vec{x},t')]$.

function is related to the reaction of the system to the external probe, say $P(\vec{x},t)$. The perturbed Hamiltonian will result in $\mathcal{H}-\int d^dxP(x,t)\phi(x,t)$, and the additional term in the Hamiltonian is tantamount to adding $P(x,t)\mu_0\tilde{\phi}(x,t)$ in the MSR action. In other words, the conjugate probe $P(x,t)\mu_0$ will couple to the response field $\tilde{\phi}(x,t)$. Intuitively, the linear response function can be defined as the ratio of the strength of the reactive field to that of the probe:

$$\begin{aligned} R_{phy}(\vec{x}-\vec{x}',t-t') &= \frac{\delta\langle\phi(x,t)\rangle}{\delta P(x',t')} \\ &= \mu_0\frac{\delta\langle\phi(x,t)\rangle}{\delta\tilde{J}(x',t')} \\ &= \mu_0\langle\phi(x,t)\tilde{\phi}(x',t')\rangle, \end{aligned} \tag{A11}$$

where $\mu_0P(\vec{x},t)=\tilde{J}(x,t)$ (note that R_{phy} is different from R_0 by a factor μ_0 and the latter is used in the calculation here). This arises from the various representations of $\tilde{\phi}$, which is associated with the unphysical degrees of freedom in multiplying the Langevin equation by an arbitrary constant.

Consistently, the response function will manifest causality. There is no response before the external probe is applied, i.e., $R(x,t)=0$ for $t<0$.

The relation between the static and the dynamic properties is through the correlation functions. In the random systems one distinguishes between equal-time correlations which correspond to the static correlations:

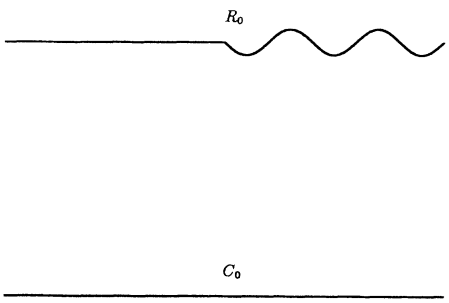

FIG. 4. The lines representing the free correlation and response functions.

$$\langle\phi(\vec{x},t)\phi(\vec{x}',t)\rangle=[\langle\phi(\vec{x})\phi(\vec{x}')\rangle]_{AV}\ , \tag{A12}$$

where $[]_{AV}$ stands for the average over disorder. In the replica calculation it is given by the diagonal term $\langle\phi_\alpha(\vec{x})\phi_\alpha(\vec{x}')\rangle$. The time-persistent part [24] of the correlation which correspond, to the Edwards-Anderson type of static correlation [25]:

$$[\langle\phi(x,t)\phi(x',t')\rangle_{t-t'\to\infty}]_{AV}=Q_{EA}(x-x'). \tag{A13}$$

In the replica language, if there is no replica-symmetry breaking, it is given by the nondiagonal part: $\lim_{n\to0}[\langle\phi^\alpha(x)\phi^\beta(x')\rangle_{\alpha\neq\beta}]_{AV}$.

APPENDIX B: PERTURBATIVE EXPANSIONS USING FEYNMAN DIAGRAMS

To facilitate the RG calculation, one can introduce 1PI (one-particle-irreducible) vertex generating functional $\Gamma[M]$. In analogy to the static case, one can define the vertex functions through Γ. For example, the vertex function $\Gamma_{1,1}$ is defined by $\frac{\delta^2\Gamma[M]}{\delta M_1\delta M_2}$ [20]. Here the calculation is focused on expanding the bare parameters. On the other hand, one also can expand the theory in terms of renormalized parameters. Up to second-order perturbation, the 1PI vertex generating functionals are expanded as [26]

$$\Gamma[M]=\frac{1}{2}(M,G_0M)+P[M], \tag{B1}$$

$$\begin{aligned} P[M] &= \langle V[\phi+M]\rangle_0-\frac{1}{2}\{\langle V^2[\phi+M]\rangle_0 \\ &\quad -\langle V[\phi+M]^2\rangle_0\} \\ &\quad -\left\{\left\langle\frac{\delta V[\phi+M]}{\delta\phi}\right\rangle_0,G_0\left\langle\frac{\delta V[\phi+M]}{\delta\phi}\right\rangle_0\right\} \\ &\quad +O(V^3), \end{aligned} \tag{B2}$$

where G_0^{-1} is symbolizing the 2×2 free propagators matrix, composed by R_0 and C_0, and the bracket $\langle\rangle_0$ stands for the average taken with respect to the free action. The second term in the right hand side of the equation is the sum of the connected diagrams up to the order of V^2, and the third term is serving to remove all connected diagrams in the second term which are not 1PIs.

To proceed with the calculations systemically, it is convenient to introduce the vertex functions here. The bare and renormalized vertex functions can be related by factors of Z_ϕ, $Z_{\tilde{\phi}}$. For instance,

$$\begin{aligned} &\Gamma^R_{N,L}(q,\omega;\lambda_R,m_R,\kappa) \\ &\quad=(Z_\phi)^{\frac{L}{2}}(\tilde{Z}_{\tilde{\phi}})^{\frac{N}{2}}\Gamma_{N,L}(q,\omega;\lambda_0,m_0,a), \end{aligned} \tag{B3}$$

where λ_R and λ_0 label renormalized parameters $(g_R,\mu,\ldots)$ and bare parameters $(g_0,\mu_0,\ldots)$, respectively. q and ω are the external momentum and frequency, respectively. In the corresponding vertex function, a is a short-distance cutoff, and κ is a mass scale. Here $\Gamma_{N,L}$

stands for the vertex function with L external ϕ lines and N external $\tilde{\phi}$ lines. The factors, Z_ϕ and $Z_{\tilde{\phi}}$, are set to remove the divergent parts of the vertex function Γ.

APPENDIX C: THE CALCULATION OF $\tilde{Z}_{\tilde{\phi}}$

Prior to the calculation, we make some remarks about the notations of the parameters. Since m_R and γ_R satisfy Eq. (19) and Eq. (20) with Z_ϕ being 1, we have $m_0 = m$ and $\gamma_0 = \gamma$. Thus there should be no confusion if we use them interchangeably.

Before entering the calculations of the Z factors, one should make reference to the relations between the various vertex functions. For the calculation of the $Z_{\tilde{\phi}}$ factor, one should focus on the vertex function [17], $\Gamma_{1,1}$. Inferred from Eq. (B3), their renormalized and bared counterparts are related by

$$\Gamma^R_{1,1}(q\omega;\mu,\nu,g) = \tilde{Z}^{1/2}_{\tilde{\phi}}\Gamma_{1,1}(q\omega;\mu_0,m_0,g_0) = \tilde{Z}^{1/2}_{\tilde{\phi}}\Gamma_{1,1}(q\omega;\mu Z^{-1}_{\tilde{\phi}},m,Z_g g). \quad \text{(C1)}$$

The contribution from the action of the first order in g to $Z_{\tilde{\phi}}$ can be calculated by considering

$$\frac{\delta^2}{\delta\tilde{M}(\vec{x},t)\delta M(\vec{0},0)}\langle V_g[\phi+M,\tilde{\phi}+\tilde{M}]\rangle, \quad \text{(C2)}$$

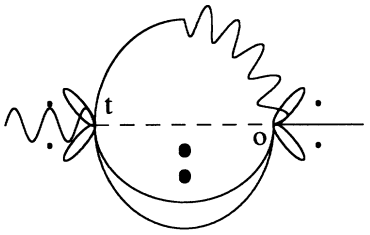

FIG. 5. The Feynman diagram for the vertex function $\Gamma_{1,1}$.

where

$$V_g[\tilde{\phi},\phi] = -\frac{\mu^2\gamma^2 g}{2a^2}\int\int d^2x dt dt' \tilde{\phi}(\vec{x},t)\tilde{\phi}(\vec{x},t') \times \cos\{\gamma[\phi(\vec{x},t)-\phi(\vec{x},t')]\}. \quad \text{(C3)}$$

Figure 5 shows one representative of the diagrams corresponding to $\Gamma_{1,1}$ in Eq. (C4). The dots inside the circle stand for the contractions of $\phi(\vec{x},t)s$ and $\phi(\vec{x},0)s$, which results in $e^{\gamma^2 C_0(0,t)}$ in Eq. (C4). The dots near the left "ears" represent the contractions of $\phi(\vec{x},t)s$ and $\phi(\vec{x},t)s$, which result in $e^{-\gamma^2 C_0(0,0)}$ in Eq. (C4). The roles of the dots near the right "ears" are similar.

In the frequency representation, the integral coming from the contractions of inner lines can be written as

$$\gamma^2\left(\int_{-\infty}^{\infty} e^{i\omega t}dtR(0,t)e^{-\gamma^2 C_0(0,0)+\gamma^2 C_0(0,t)} - (i\omega)\frac{1}{\mu^2 D}\int_0^\infty dt e^{i\omega t}e^{-\gamma^2 C_0(0,0)}\right) \quad \text{(C4)}$$

$$= e^{-\gamma^2 C_0(0,0)}\int_0^\infty dt e^{i\omega t}dt\frac{1}{\mu^2 D}\frac{d}{dt}\gamma^2 C_0(0,t)[e^{\gamma^2 C_0(0,t)}-1]$$

$$= e^{-\gamma^2 C_0(0,0)}i\omega\int_0^\infty dt e^{i\omega t}[e^{\gamma^2 C_0(0,t)}-1]\left(\frac{1}{\mu^2 D}\right). \quad \text{(C5)}$$

Combining with the prefactors and using $g = g_0(cm^2a^2)^\delta$, we have

$$(-i\omega)\gamma^2 cm^2\frac{\mu_0^2}{\mu_0^2 D_0}g\int_{a^2/\lambda}^{1/m^2\lambda}\frac{dt}{2\sqrt{cm^2\mu_0 t}}. \quad \text{(C6)}$$

Finally, $\tilde{Z}_{\tilde{\phi}}$ is found as

$$\tilde{Z}_{\tilde{\phi}} = 1 + \frac{g\gamma^2\sqrt{c}}{2*(\mu D)}\ln(\kappa^2 a^2), \quad \text{(C7)}$$

where $\kappa = cm^2$ is the scale at which one can impose the prescription for the vertex functions corresponding to the renormalized parameters [26].

APPENDIX D: THE CALCULATION OF Z_D

To calculate the factor Z_D, we consider the vertex function $\Gamma_{2,0}$. The bare vertex function $\Gamma_{2,0}$ is related to $\Gamma^R_{2,0}$ through $Z_{\tilde{\phi}}$. They can easily be seen from Eq. (B3):

$$\Gamma^R_{2,0}(\vec{q},\omega;\mu,g) = \tilde{Z}_{\tilde{\phi}}\Gamma^0_{2,0}(\vec{q},\omega;\tilde{Z}_{\tilde{\phi}}\mu,Z_g g). \quad \text{(D1)}$$

The associated diagram is illustrated in Fig. 6. After taking the contraction of the inner lines, we are left with

$$-\frac{g\mu_0^2\gamma_0^2}{2a^2}\int\int\tilde{M}(x,t')\tilde{M}(x,t), \quad \text{(D2)}$$

times $2\langle\cos\{\gamma[\phi(x,t)-\phi(x,t')]\}\rangle_0$, where the contents inside the angle brackets are averaged with respect to the free action. The latter term contributes to the renormalization of the two-point vertex depicted in Fig. 6. The calculation of this term can be performed with ease as shown below. In the time representation, it reads

$$-2\frac{g\mu_0^2\gamma_0^2}{2a^2}e^{-\gamma^2 C_0(0,0)}\int_{-\infty}^{\infty}dt e^{\gamma^2 C_0(0,t)}e^{i\omega t}. \quad \text{(D3)}$$

In the limit $\omega \to 0$, it reduces to

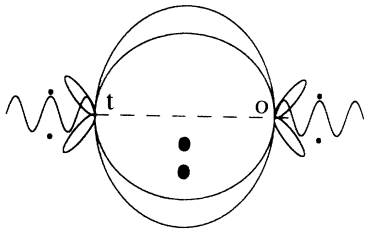

FIG. 6. The Feynman diagram for the vertex function $\Gamma_{2,0}$.

$$-2\frac{g\mu_0^2\gamma_0^2}{2a^2}e^{-\gamma^2 C_0(0,0)}\int_{-\infty}^{\infty}dt e^{\gamma^2 C_0(0,t)}. \quad \text{(D4)}$$

With the aid of the formula given in Appendix A, the divergent part of this term can be obtained by proceeding in the same manner as in the preceding section:

$$-2\frac{g\mu_0^2\gamma_0^2}{2a^2}e^{-\gamma^2 C_0(0,0)}\frac{-2}{2\sqrt{c}m^2\mu}\ln(cm^2a^2)+\text{finite terms}. \quad \text{(D5)}$$

Then,

$$-2D\mu^2=(\tilde{Z}_{\tilde{\phi}})^2\{-2D_0\mu_0^2+\gamma^2\sqrt{c}g\mu_0\ln(cm^2a^2)\}. \quad \text{(D6)}$$

Finally we inherit $Z_D = 1+\frac{\gamma^2\sqrt{c}g}{2D\mu}\ln(cm^2a^2)$. There should be no confusion if we put either the bare or the renormalized values of D and μ in the denominator in the above equation. Up to this order, there will be no difference between these two possibilities.

APPENDIX E: THE EXPRESSION OF Z_g AND THE RENORMALIZATION OF $\bar{\nu}$

It is a tedious calculation to find Z_g by considering the vertex function $\Gamma_{2,0}(\vec{q},\omega)$. Since quenched disorder is present in the system, one may instead consider $\Gamma_{2,0}(\vec{q},t_1;-\vec{q},t_2)$, in the limit $|t_1-t_2|\to\infty$.

To obtain the scaling equation of $\bar{\nu}$, one should consider the $\vec{q}$-dependent part of $\Gamma_{2,0}(\vec{q},t_1;-\vec{q},t_2)$ with $|t_1-t_2|\to\infty$. The contractions of fields which connect the points t_1 and t_2 make no contributions. The $\vec{q}$-dependent part of $\Gamma_{2,0}$ up to order g^2 involves seven diagrams, which are classified into three sets as illustrated in GS [17]. Those terms can be expressed as the first seven terms in (7.3) of GS [17]. The first set [referred to Fig. 1(a) in GS] contains only one diagram, as shown in Fig. 7(A). The

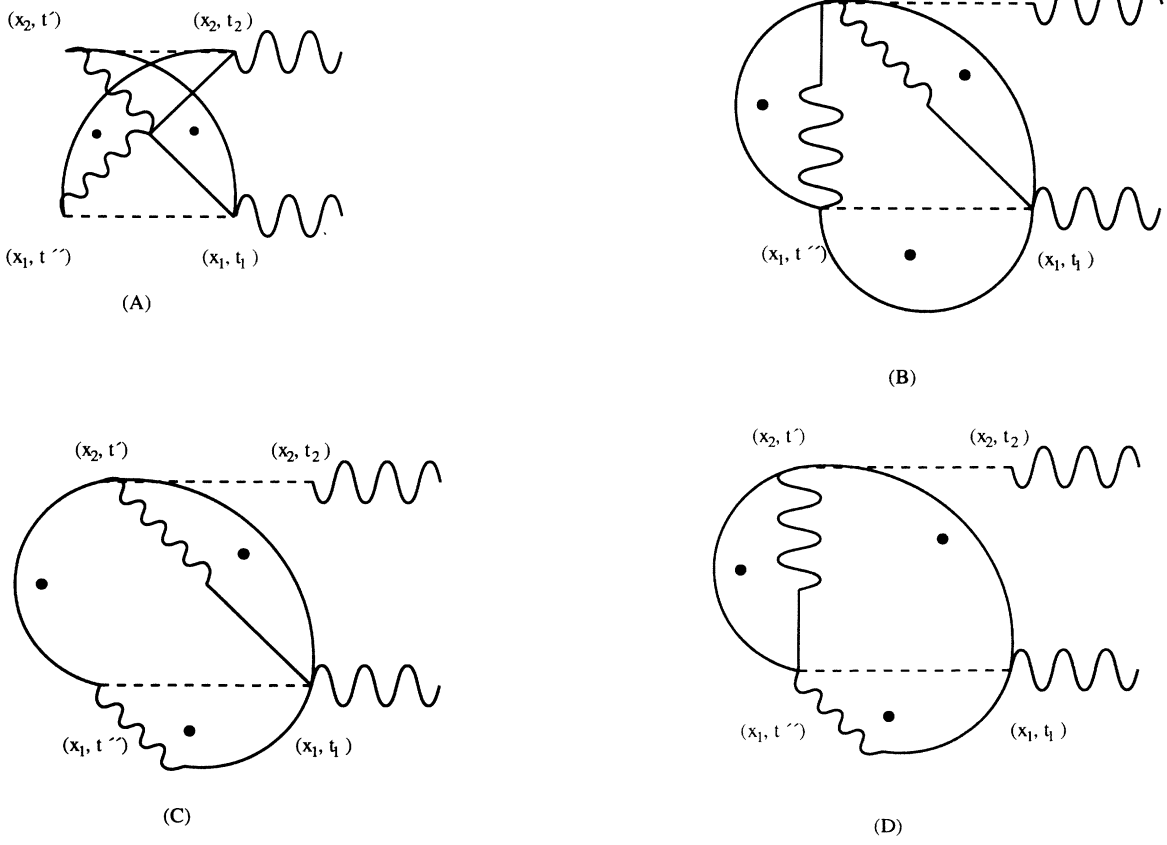

FIG. 7. Four Feynman diagrams contributing to the renormalization of $\bar{\nu}$.

second set contains three diagrams, corresponding to (B), (C), and (D) in Fig. 7. The third set can be obtained from the second set by swapping $(x_1,t_1) \longleftrightarrow (x_2,t_2)$ and $(x_1,t'') \longleftrightarrow (x_2,t')$.

In the following, we only present the calculations which are not explicitly given in GS [17]. In the calculation, we only concentrate on the time-dependent part, neglecting the prefactors. This should not be a cause for confusion when one retrieves them later. By changing the variables $\tau' = t_1 - t'$ and $\tau'' = t_2 - t''$ the first term is recast into

$$\int_{-\infty}^{\infty} d\tau' \int_{-\infty}^{\infty} d\tau'' R_0(x,\tau') R_0(x,\tau'') \times \sinh\gamma^2[-C_0(x,\tau') - C_0(x,\tau'')], \quad \text{(E1)}$$

where $x = x_1 - x_2$.

With the identity of FDT for R_0 and C_0 and the integration by parts, it is simplified into

$$\frac{-1}{(\mu^2 D\gamma^2)^2} \int_0^{\infty} \int_0^{\infty} d\tau' d\tau'' \left\{ \left(\frac{d}{d\tau'} \sinh\gamma^2 C_0(x,\tau')\right) \left(\frac{d}{d\tau''} \cosh\gamma^2 C_0(x,\tau'')\right) + \left(\frac{d}{d\tau'} \cosh\gamma^2 C_0(x,\tau')\right) \left(\frac{d}{d\tau''} \sinh\gamma^2 C_0(x,\tau'')\right) \right\} = \frac{-2}{(\mu^2 D\gamma^2)^2} \sinh[\gamma^2 C_0(x,0)]\{\cosh[\gamma^2 C_0(x,0)] - 1\}. \quad \text{(E2)}$$

By changing the variables $\tau' = t_1 - t'$ and $\tau'' = t' - t''$ in the second term [see part (B) in Fig. 7] and $\tau' = t'' - t'$ and $\tau'' = t_2 - t''$ in the fifth term, they become

$$-\int_{-\infty}^{\infty} d\tau' \int_{-\infty}^{\infty} d\tau'' R_0(x,\tau') R_0(x,\tau'') \exp[\gamma^2 C_0(0,\tau'+\tau'')] \sinh\gamma^2[C_0(x,\tau') - C_0(x,\tau'')]. \quad \text{(E3)}$$

By changing the variables $\tau' = t_1 - t'$ and $\tau'' = t' - t''$ in the third term [see part (C) in Fig. 7] and $\tau' = t_2 - t''$ and $\tau'' = t'' - t'$ in the sixth term, they become

$$-\int_{-\infty}^{\infty} d\tau' \int_{-\infty}^{\infty} d\tau'' R_0(x,\tau') R_0(0,\tau'+\tau'') \exp[\gamma^2 C_0(0,\tau'+\tau'')] \cosh\gamma^2[C_0(x,\tau') - C_0(x,\tau'')]. \quad \text{(E4)}$$

By changing the variables $\tau' = t'' - t'$ and $\tau'' = t' - t_1$ in the fourth term [see part (D) in Fig. 7] and $\tau' = t' - t''$ and $\tau'' = t'' - t_2$ in the seventh term, they become

$$\int_{-\infty}^{\infty} d\tau' \int_{-\infty}^{\infty} d\tau'' R_0(x,\tau') R_0(0,-\tau'-\tau'') \exp[\gamma^2 C_0(0,\tau'+\tau'')] \cosh\gamma^2[C_0(x,\tau') - C_0(x,\tau'')]. \quad \text{(E5)}$$

With the FDT identity, Eq. (E3) can be futher simplified into

$$-\frac{1}{(\mu^2 D\gamma^2)^2} \int_0^{\infty} d\tau' \int_0^{\infty} d\tau'' \exp[\gamma^2 C_0(0,\tau'+\tau'')] \left(\frac{d}{d\tau'} \cosh\gamma^2 C_0(x,\tau') \frac{d}{d\tau''} \sinh\gamma^2 C_0(x,\tau'') - \frac{d}{d\tau''} \cosh\gamma^2 C_0(x,\tau'') \frac{d}{d\tau'} \sinh\gamma^2 C_0(x,\tau') \right). \quad \text{(E6)}$$

By using the FDT and the integration by parts, one can reduce Eq. (E4) into

$$\frac{1}{(\mu^2 D\gamma^2)^2} \int_0^{\infty} d\tau' \int_{-\tau'}^{\infty} d\tau'' \exp[\gamma^2 C_0(0,\tau'+\tau'')] \left(\frac{d}{d\tau'} \cosh\gamma^2 C_0(x,\tau') \frac{d}{d\tau''} \sinh\gamma^2 C_0(x,\tau'') - \frac{d}{d\tau''} \cosh\gamma^2 C_0(x,\tau'') \frac{d}{d\tau'} \sinh\gamma^2 C_0(x,\tau') \right) + \text{the boundary term} . \quad \text{(E7)}$$

Similiarly, Eq. (E5) is recast into

$$\frac{1}{(\mu^2 D\gamma^2)^2}\int_0^\infty d\tau' \int_{-\infty}^{-\tau'} d\tau'' \exp[\gamma^2 C_0(0,\tau'+\tau'')]\left(\frac{d}{d\tau'}\cosh\gamma^2 C_0(x,\tau')\frac{d}{d\tau''}\sinh\gamma^2 C_0(x,\tau'')\right.$$

$$\left.-\frac{d}{d\tau''}\cosh\gamma^2 C_0(x,\tau'')\frac{d}{d\tau'}\sinh\gamma^2 C_0(x,\tau')\right) + \text{the boundary term} . \quad \text{(E8)}$$

Combining Eq. (E6), Eq. (E7), and Eq. (E8) terms excluding the boundary terms, we have

$$\frac{1}{(\mu^2 D\gamma^2)^2}\int_0^\infty d\tau' \int_{-\infty}^{0} d\tau'' \exp[\gamma^2 C_0(0,\tau'+\tau'')]\left(\frac{d}{d\tau'}\cosh\gamma^2 C_0(x,\tau')\frac{d}{d\tau''}\sinh\gamma^2 C_0(x,\tau'')\right.$$

$$\left.-\frac{d}{d\tau''}\cosh\gamma^2 C_0(x,\tau'')\frac{d}{d\tau'}\sinh\gamma^2 C_0(x,\tau')\right). \quad \text{(E9)}$$

The above integral vanishes since the integrand is antisymmetric with respect to the transformations $\tau' \to -\tau''$ and $\tau'' \to -\tau'$.

The boundary terms in Eq. (E4) and in Eq. (E5) cancel each other also. For example, the boundary term in Eq. (E4) reads as

$$\int_0^\infty d\tau' \frac{d}{d\tau'}[\sinh\gamma^2 C_0(x,\tau')] + \int_0^\infty d\tau' \exp[\gamma^2 C_0(0,0)]$$

$$\times\left(\frac{d}{d\tau'}\sinh\gamma^2 C_0(x,\tau')\cosh\gamma^2 C_0(x,-\tau') - \frac{d}{d\tau'}\cosh\gamma^2(x,\tau')\sinh\gamma^2 C_0(x,-\tau')\right). \quad \text{(E10)}$$

To sum up, the only contribution is from Eq. (E2). Extracting the singular contribution [17,19] gives $\bar{\nu}_b = \bar{\nu} + \frac{\gamma^2 g^2}{8\pi(D\mu)^2}\ln(\kappa^2 a^2)$.

[1] For a recent review, see H. van Beijeren and I. Nolden, in *Structure and Dynamics of Surface II*, edited by W. Schommers and P. von Blackenhagen (Springer-Verlag, Berlin, 1987).

[2] For reviews of recent experimental and theoretical developments see, e.g., *Kinetics of Ordering and Growth at Surfaces*, edited by M. Lagally (Plenum, New York, 1990); *Dynamics of Fractal Surfaces*, edited by F. Family and T. Vicsek (World Scientific, Singapore, 1991), and references therein.

[3] For a review, see, e.g., J. Krug and H. Spohn, in *Solids Far from Equilibrium*, edited by C. Godreche (Cambridge University Press, Cambridge, England, 1991).

[4] S. T. Chui and J. D. Weeks, Phys. Rev. Lett. **40**, 733 (1978).

[5] P. Nozieres and F. Gallet, J. Phys. (Paris) **48**, 353 (1987).

[6] Y. C. Tsai and Y. Shapir, Phys. Rev. Lett. **69**, 1773 (1992).

[7] P. C. Martin, E. Siggia, and H. Rose, Phys. Rev. A **8**, 423 (1973).

[8] S. K. Ma and G. F. Mazenko, Phys. Rev. B **11**, 4077 (1975).

[9] S. K. Ma, *Modern Theory of Critical Phenomena* (W. A. Benjamin, New York, 1976); D. Forster, *Hydrodynamic Fluctuation, Broken Symmetry, and Correlation Functions* (W. A. Benjamin, New York, 1975); L. E. Reichl, *A Modern Course in Statistical Physics* (University of Texas Press, Austin, 1980).

[10] M. Kardar, G. Parisi, and Y. C. Zhang, Phys. Rev. Lett. **56**, 889 (1986); E. Medina, T. Hwa, M. Kardar, and Y. C. Zhang, Phys. Rev. A **39**, 3053 (1989).

[11] M. P. A. Fisher, Phys. Rev. Lett. **62**, 1415 (1989).

[12] D. S. Fisher, M. P. A. Fisher, and D. A. Huse, Phys. Rev. B **43**, 130 (1990).

[13] T. Nattermann, I. Lyuksyutov, and M. Schwartz, Europhys. Lett. **16**, 295 (1991); T. Nattermann and I. Lyuksyutov, Phys. Rev. Lett. **68**, 3366 (1992).

[14] Y. Shapir and Y. C. Tsai, Phys. Rev. Lett. **71**, 2348 (1993).

[15] S. Edwards and D. R. Wilkinson, Proc. R. Soc. London, Ser. A **381**, 17 (1982).

[16] D. J. Amit, Y. Y. Goldschmidt, and G. J. Grinstein, J. Phys. A **13**, 585 (1980).

[17] Y. Y. Goldschmidt and B. Schaub, Nucl. Phys. **B251**, 77 (1985).

[18] J. Zinn-Justin, *Quantum Field Theory and Critical Phenomena* (Oxford University Press, New York, 1989).

[19] D. J. Amit, *Field Theory, the Renormalization Group, and Critical Phenomena* (World Scientific, Singapore, 1984).

[20] H. K. Janssen, Z. Phys. B **23**, 377 (1976); B. Bausch, H. K. Janssen, and H. Wanger, *ibid.* **24**, 113 (1976); C. De

Dominicis and L. Peliti, Phys. Rev. B **18**, 353 (1978).
[21] J. Toner and D. P. DiVincenzo, Phys. Rev. B **41**, 632 (1990).
[22] J. Toner, Phys. Rev. Lett. **67**, 2537 (1991); **68**, 3367 (1992).
[23] S. E. Korshunov, Phys. Rev. B **48**, 3969 (1993); T. Giamarchi and P. LeDoussal, Phys. Rev. Lett. **72**, 1530 (1994).
[24] C. De Dominicis, Phys. Rev. B **18**, 4913 (1978).
[25] For a review, see K. Binder and A. P. Young, Rev. Mod. Phys. **58**, 801 (1986); and M. Mézard, G. Parisi, and M. A. Virasoro, *Spin Glass Theory and Beyond* (World Scientific, Singapore, 1987).
[26] B. Neudecker, Z. Phys. B **49**, 57 (1982); **48**, 149 (1982).
[27] G. G. Batrouni and T. Hwa, Phys. Rev. Lett. **72**, 4133 (1994).
[28] D. Cule and Y. Shapir (unpublished).